Journal of Materials Chemistry C

ROYAL SOCIETY OF CHEMISTRY

REVIEW

View Article Online
View Journal | View Issue

Cite this: J. Mater. Chem. C, 2020, 8, 12036

Recent developments of colorimetric mechanical sensors based on polymer composites

Ezgi Inci, [a] Gokhan Topcu, [b] Tugrul Guner, [c] Merve Demirkurt[d] and Mustafa M. Demir *[a]

Received 31st May 2020,
Accepted 28th July 2020

DOI: 10.1039/d0tc02600j

rsc.li/materials-c

Colorimetric mechanical (force, pressure, strain, and impact) sensors allow naked-eye visualization of existing structural deformations of a system occurring upon application of a mechanical action. The combination of mechanochromic materials with polymers offers a practical approach to designing and fabricating these sensors. Polymers as matrices can tolerate a wide range of forces and permits reusability of the sensors. On the other hand, mechanochromic materials provide unique colour properties depending on the type of mechanical action. They have also been frequently employed for the quantification of mechanical forces. As an example, non-centrosymmetric crystals are combined with polymers for sensing impact forces. Structures with photoluminescence and scattering and plasmonic resonances can be used to fabricate strain and pressure responsive composite materials, respectively. This study reviews recent advances in colorimetric mechanical sensor systems prepared using polymers and inorganic and organic mechanochromic materials working under a wide range of forces.

1 Background

Colorimetric optical signals initiate natural activities in wildlife such as mating, hunting, and combat.[1–7] This phenomenon has inspired researchers to develop bio-inspired functional materials[8–10] that change colour upon exposure to an external stimulus such as mechanical action. A mechanical force is converted into an optical signal through a process called mechanochromism. While commercially available mechanical sensors are mainly based on electronic systems that need additional and exclusive circuitry assembly,[11] colorimetric mechanical sensors exhibit a visible optical response upon application of mechanical action.[12–16] They offer various advantages such as being cost-effective and easy detection of stimuli even by the naked eye.[17] These sensors find essential application in strain, impact, and damage indicators in biomedical devices, smart displays, household products, fingerprint identification, and civil engineering.[18] Moreover, colorimetric mechanosensors have received a great deal of interest due to their strong ability to control light propagation, vivid color display, and zero energy consumption.[19] As in all sensor technologies, sensitivity, selectivity and rapid detection are major challenges to colorimetric mechanical sensors. Despite these obstacles, colorimetric sensors have become widely accepted in many daily life applications. Mixing polymers and mechanochromic additives is a versatile approach to obtain flexible and processible stimuli responsive materials.[20] Mechanochromic materials that reversibly or

[a] Department of Materials Science and Engineering, İzmir Institute of Technology, Gülbahçe, Urla, İzmir, 35430, Turkey. E-mail: mdemir@iyte.edu.tr; Fax: +90 232 750 7509; Tel: +90 232 750 7511
[b] Chemistry Department, Koç University, Sarıyer, 34450, İstanbul, Turkey
[c] Centre Energie, Matériaux et Télécommunications, Institut National de la Recherche Scientifique (INRS), Montreal, QC J3X 1S2, Canada
[d] Kanat Paints & Coatings, Kemalpaşa OSB 321, İzmir, Turkey

Ezgi Inci received her BSc in Materials Science and Engineering (2017) from Anadolu University and MSc in Materials Science and Engineering (2019) from the İzmir Institute of Technology. She has been carrying out her PhD on inorganic nanomaterials and polymeric composites in the Department of Materials Science and Engineering in the İzmir Institute of Technology since September 2019. Her current research is on the fabrication of Langmuir–Blodgett coatings and mechanical sensors.

Gokhan Topcu received his BSc in Chemistry (2013) and MSc in Organic Chemistry (2015) from Marmara University. He completed his doctoral research on the development of mechanical sensors by using plasmonic and photonic nanostructures in polymeric systems in the Department of Materials Science and Engineering in the İzmir Institute of Technology (2019). He is currently a postdoctoral researcher at Koç University and continues his research studies on advanced polymeric composites and physical interactions/self-assembly of macromolecules.

permanently change their colour as a response to external stimuli are of widespread fundamental importance.[21] In general, these optically active functional additives are mostly inorganic/organic and/or organometallic compounds.[22] Their sole use leads to restrictions in sensor applications due to their inherent rigidity, hard processing conditions, and discontinuity.[23] Therefore, polymeric composites thereof provide tailorable colorimetric properties owing to their versatility, processability, and reusability in the visible region.[24,25] In this context, the nature of polymers in such composite sensors has a dramatic role and their physical properties need to be considered for careful design. For instance, the responsivity is related to the transparency of matrices since it can facilitate light propagation, namely the signal output of colorimetric sensors. Both the optical properties and mechanical behaviour of polymeric matrices have strong influences on the reversibility and reusability of mechanochromic systems. The polymeric materials employed in mechanochromic composites behave like rubber or elastomers and exhibit almost complete reversibility.[26] In contrast, the use of viscoelastic polymers causes irreversible responses, yet the polymers may preserve the colorimetric data even after removing the stimulus. Moreover, the low cost, processability, and mechanical robustness of polymer matrices make them useful and good candidates for long-term use.[27]

Over the past few decades, various polymer composites have been fabricated that show optical response to stimuli such as force, temperature, chemical substances, and pH using various chemical and nanostructure systems.[20,28–32] Literature examples are compiled in Table 1, along with the types of mechanochromic additives, the types of polymers and the corresponding preparation methods. Mechanical deformation and the range of mechanical action are also presented. The underlying mechanism is important for selection of mechanochromic materials, which can be summarized under four different optical phenomena (Scheme 1).

Triboluminescence (TL), namely luminescence generated through crack or fracture formation under mechanical actions, can serve as an example of emission related optical responses.[33,34] The combination of TL materials with an elastic matrix allows the transfer of this optical feature to the matrix material. If a careful calibration curve is prepared, one can obtain information about the magnitude of the applied impact using the intensity of the TL emission. The shift of the emission signal at the excitation wavelength (photoluminescence) upon application of a mechanical action can be another source of mechanochromism. This change usually occurs due to the switching of the molecular structure, conformational rearrangements and/or intermolecular interactions.[35–37] Photonic crystals are also a candidate for mechanochromic materials.[38–41] Numerous polymer-based three-dimensional photonic crystalline structures that show responsive colour change upon stretching have been developed.[18,42–45] Diffraction, *i.e.* a coherent scattering of incident light from periodic structures, generates colours; the variation of periodicity upon application of a mechanical action causes a change in colorimetry. The sensitivity of a sensor system can be determined by the shift in the reflectance spectrum divided by the applied strain.[46] Along with sensor applications, these responsive photonic crystal composites have remarkable potential in colour displays, inks and paints, and numerous optically active components.[42] Moreover, some metal nanoparticles with surface plasmons such as Au and Ag can be sources of mechanochromic materials.[47,48] The plasmon resonance of the coupled particles depends on the interparticle distance.[49–52] Therefore, assembly/disassembly of the particles causes a strong plasmonic signal and distinct colour change. Such plasmonic nanoparticles may respond to mechanical actions or even influence the optical processes of molecules present on their surfaces (*e.g.*, absorption, fluorescence, and Raman scattering).[53] Metal nanoparticles are embedded into polymers to contribute optical response to generate colorimetric mechanical sensors.[54–56]

The aim of this review is to give a general picture of the fundamentals of colorimetric mechanical sensors from the perspectives of preparation methods, sensing performance, and further potential applications. This part of the text includes basic statistical data from the literature. A brief summary of the preparation methods of sensor systems and key applications of colorimetric mechanical sensors will be given further in the text, while expatiating on the state of the art of these materials.

Tugrul Guner received his BSc in Physics (2011) from Bilkent University, MSc in Physics (2015) from the Izmir Institute of Technology, and PhD in Materials Science and Engineering (2018) from the Izmir Institute of Technology. He studied down-converting materials and their white light applications during his doctoral thesis. He is currently a postdoctoral fellow in the Centre Énergie Matériaux Télécommunications (EMT) at the Institut National de la Recherche Scientifique (INRS) in Quebec (Canada), and he is currently conducting research studies on the understanding and imaging of the ultrafast dynamics of nanomaterials using ultrafast transmission electron microscopy.

Merve Demirkurt received her BSc (2008) and MSc (2011) in chemistry from the Izmir Institute of Technology. She completed her doctoral thesis on synthesis of novel molecularly imprinted polymers and various functionalized nanomaterials for determination of endocrine disrupting compounds by chromatographic analysis. She is currently a senior R&D chemist at Kanat Paints and Coatings and continues her research on smart coating systems.

Mustafa M. Demir is Professor at the Izmir Institute of Technology, Department of Materials Science and Engineering. He coordinates an interdisciplinary group working on synthesis and nanotechnologies on soft matter. His research activity is focused on the development of polymeric optical nanocomposites for advanced applications, electrospinning, and functional systems. He was awarded the "Young Researcher" Prize of the Turkish Academy of Sciences in 2013. His details can be found at: http://www.demirlab.iyte.edu.tr.

Table 1 Overview of mechanochromic materials and their working ranges in the literature

Polymer matrix	Chromic additive	Processing technique	Type of stimulus	Properties	Reversibility	Ref.
PVDF	EuD_4TEA	Spin coating	Impact	Force range = 5.4–9.5 N	Irreversible	57
PDMS	$ZnS:M^{2+}$(Mn/Cu)@ Al_2O_3	Dispersion and printing processes	Impact	A strain of 20% at a frequency at 2 Hz	Reversible	58
PU	EuD_4TEA	Blending in solution or surface impregnation	Impact	Force range = 2.45–42.00 N	Irreversible	59
PU	$Cu(NCS)(py)_2(PPh_3)$	Surface impregnation on nonwoven electrospun mats	Impact	Force range = 0.98–4.98 N	Irreversible	60
LLDPE	Cyano-OPVs = BCMDB and BCMB	Conventional melt processing	Strain	Stretching ratio = 500%	Irreversible	61
PU	Cyano-OPVs = C1-RG, C18-RG	Conventional melt processing	Strain	Stretching ratio = 200–300%	Irreversible	62
Polyamide 12	C18-RG	Conventional melt processing	Strain	Stretching = 80%	Reversible	63
PDMS	(PVA)/LAPONITE® composite	Drop casting, spray coating, curing	Strain	Strain range = 0–40%	Reversible	64
PDMS PVA	$Y_2O_3:Eu_3$ TiO_2	Drop casting, spray coating, curing	Strain	Strain range = 0–20%	Reversible	64
PDMS	SiO_2 particles	Spray coating, curing	Strain	Strain range = 0–80%	Reversible	65
PDMS	PS particles	Drop casting	Strain	Strain range = 0–20%	Reversible	66
pPEGPEA	SiO_2 particles	Photopolymerization	Strain	Strain range = 20–47%	Reversible	40
Poly(ethyl acrylate)	Colloidal particles MMA and ethyl acrylate	Soap-free emulsion polymerization	Strain	Poisson's ratio = 0.497 (rubbery soft materials $\approx$ 0.5)	Reversible	41
pPEGPEA	SiO_2 particles	Photopolymerization	Strain	Strain range = 0–50%	Reversible	39
PVP PEG	Au NPs	Dispersion and drop casting	Pressure	Pressure range = 7×10^3–1.6×10^5 psi Expansion up to 66% with PEG doping	Irreversible	67
PAAm	Au NPs	Dispersion and drop casting	Pressure	Pressure range up to 160 MPa	Irreversible	55

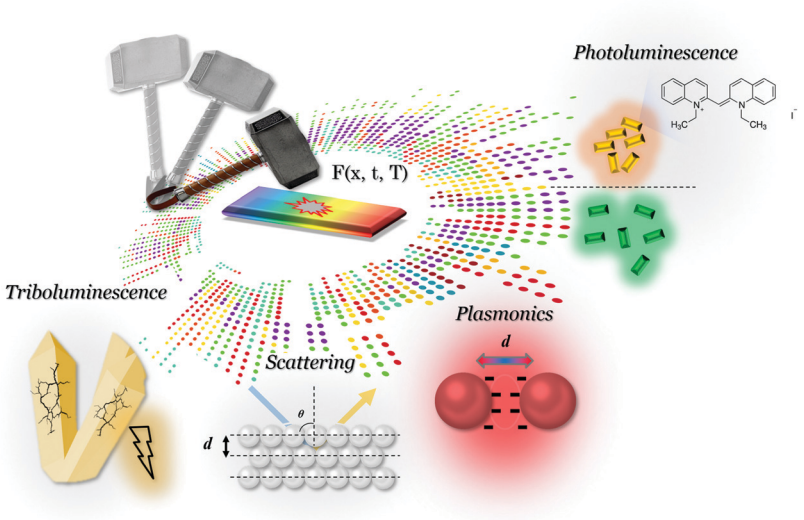

Scheme 1 Schematic outlook for reviewed mechanochromic sensors governed by different mechanisms.

From this starting point, the rational design and fabrication of polymeric mechanical sensors working under a wide range of external mechanical forces with various tones of colours may become possible.

To study the development of these subjects, publications were collected and classified with respect to their publication year using the Web of Science with keywords "photoluminescence," "plasmonics," "triboluminescence," and "light scattering." Moreover, sensor and mechanochromic sensor related publications were extracted from these datasets as subsets by searching for "sensor" and "sensor" + "mechanical" (meaning that "mechanical" was extracted from "sensor" related publications) keywords. Publication years were classified into three groups in order to see the distribution of publications over certain year ranges: before 2000 as "<2000" to represent old publications, between 2000 and 2010 as "2000–2010", and after 2010 as

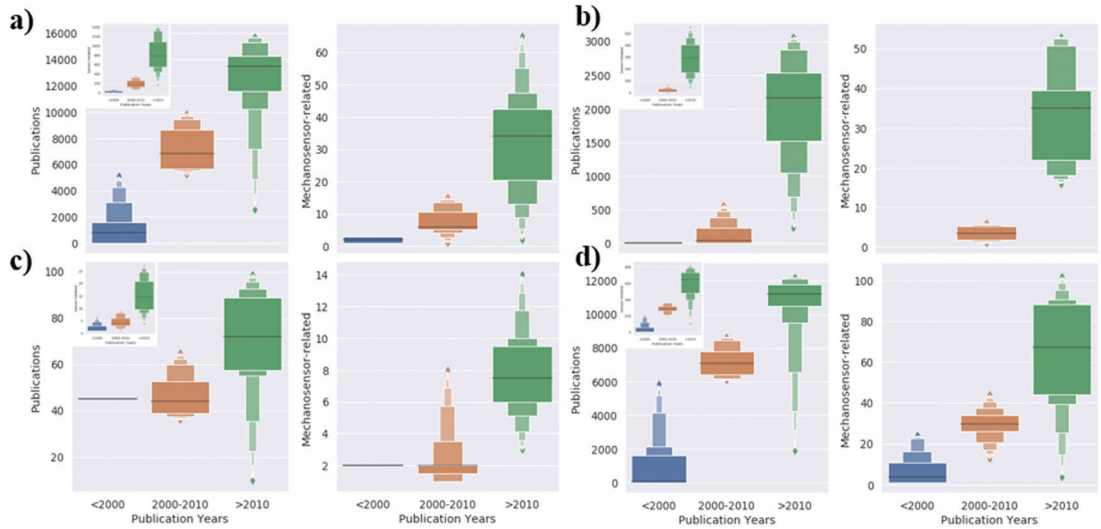

Fig. 1 Statistical distributions of (a) photoluminescence, (b) plasmonics, (c) triboluminescence, and (d) light scattering publications with respect to publication years classified into certain time periods such as before 2000 (<2000), between 2000 and 2010 (2000–2010), and after 2010 (>2010). In each part, the first figure shows total publications, while the inset demonstrates sensor-related ones, and the second figure illustrates mechanochromic sensor-related publications.

">2010." Processed data were plotted (Fig. 1) using "letter value plots" *via* the Seaborn python library.[68,69] Here, the black lines for each distribution represent the medians of the data. The box height indicates the corresponding range of lower and upper hinges as interquartile regions. The algorithm first draw the largest box around median. Then it continues to find interquartile regions for each remaining data distribution and draw smaller boxes. The reduction of the box width continuous many times until whole data is covered (data that remain outside of the box/boxes in both the upper and lower regions separately). Therefore, the box size hints about how far it is from the central distribution, as an outlier. The left panels represent total general publications with main keywords from (a) to (d) in the same order as above. Inset plots demonstrate sensor related publications, while the right figures illustrate mechanochromic sensor related ones. All these plots suggest that the general trends for the publications in these fields (taking black lines into account) have reached their peak in recent years, indicating that there has been growing interest over time. More specifically, Fig. 1a shows that before 2000 photoluminescence publications were around 1000, while after 2010 they reached 13 000, which constitutes a dramatic increase. Similarly, sensor and mechanochromic related publications jumped from almost 0 to 800 and 0 to 35, respectively. In the case of plasmonics, Fig. 1b, the numbers of publications in <2000 and 2000–2010 were similar, but after 2010 the number has increased dramatically to 2250. Since this is a new field which emerged mostly with the advances of nanotechnology, there were almost no publications before 2010. After 2010, sensor and mechanochromic sensor related publications have reached 300 and 35, respectively. Meanwhile, although TL has been known for a long time, the number of related publications is relatively low, around 45 before 2000 and between 2000 and 2010. However, after 2010, there has also been a significant increase in TL papers, reaching 70 but with a maximum of 100. Sensor related papers show an increasing trend over these time ranges, from 2 to 4 and then 15, respectively, while mechanochromic sensor related ones started to jump after 2010, increasing from 2 to 8. Light scattering publications were numerous before 2000 but had a median below 1000 and increased dramatically between the years 2000 and 2010, reaching almost 11 000 publications after 2010. Similarly, sensor and mechanochromic sensor related publications have demonstrated an increasing trend over time, increasing from almost 0 for both to 700 and 70 publications, respectively. As a result, these fields will attract more attention in the near future, and we expect that mechanochromic related publications, as subsets of these fields, will continue to grow.

2 Triboluminescence

TL is a term used to define a flash of light produced by materials as a result of impact or under any mechanical action. It may be one of the oldest known sources of luminescence. Even though the first examples of its application originated from the Uncompahgre Ute Indians from Central Colorado,[70] the first recorded discovery of its presence dates back to the beginning of the 17th century. It was reported in the Advancement of Learning by Francis Bacon based on his observations from scraped sugar.[71] Since then, contributions to this field had mainly focused on the discovery of different types of TL materials from inorganic to organic crystals until the 19th century. Finally, systematic studies exploring the physical mechanisms behind this phenomenon and revealing the relationship between crystal structures and TL appeared in the 20th century thanks to advancements in instrumentation to catch up weak and short life time signals.[72] Even though some satisfactory physical mechanisms have so far been proposed to explain the source of radiation in these materials, they work

well in only certain cases, meaning that TL is still short of a universal theory.[73]

One of the well-known explanations for TL was proposed by Langevin in 1913[74] and further elucidated by Longchambon,[75,76] which took into consideration oppositely charged fracture planes appearing in almost all non-centrosymmetric crystals. The electric field between these planes causes gas-discharge and therefore results in an emission due to the energy released from neutralized ions while returning to the lower energy state. Fig. 2 presents how a typical fractured crystal reorganizes the charge distributions in cracked regions by forming oppositely charged planes in this model that create emission based on gas-discharge. First, under certain stress, the system has positive and negative charge distributions due to its piezo nature (Fig. 2a). A crack or fracture emerges in the system as the applied stress changes, which causes reorganization of the charge distribution between the fractured regions (Fig. 2b). During this process, gas-discharge occurs and results in luminescence. A typical TL spectrum for gas-discharge is usually related to characteristic N_2 emission. For instance, sucrose[77,78] and $Li_2SO_4{\cdot}H_2O$[74] demonstrate this characteristic TL emission (Fig. 2c). However, this explanation fails in the case when emission does not match with the surrounding particular gas emission spectrum[79] or when the TL material is a non-piezoelectric crystal. For instance, europium tetrakis(dibenzoylmethide) triethylammonium (EuD_4TEA) crystals show typical Eu^{3+} ion spectral distribution instead of indicating any characteristic emission spectrum of the surrounding gases.[80,81] On the other hand, some well-known statistics about materials with centrosymmetry, such as 68% of aromatic organic compounds,[82] 53% of inorganic sulfates,[78] 73% of triclinic crystals,[83,84] and 50% of nitrates and halogens,[85] reveal that a significant amount of non-piezoelectric crystals can exhibit TL.[86] Nevertheless, TL started to get more attention with advancements in sensor technologies, such as real-time sensors and mechano-sensors, and in bio-imaging devices, display technologies, *etc.* To gain further insight into the details of TL for non-piezoelectric crystals, various mechanisms have been proposed including impurity/defect or fracture induced local piezoelectric fields, electron bombardment, and charge dislocations or disorder in materials.[71,77,87] For more details about the proposed mechanisms and TL applications, readers are strongly encouraged to refer to some recent reviews.[88–90] Here, we will focus mainly on applications of TL materials in the form of polymer composites as mechanochromic sensors, in other words, transfer of TL to polymeric systems.

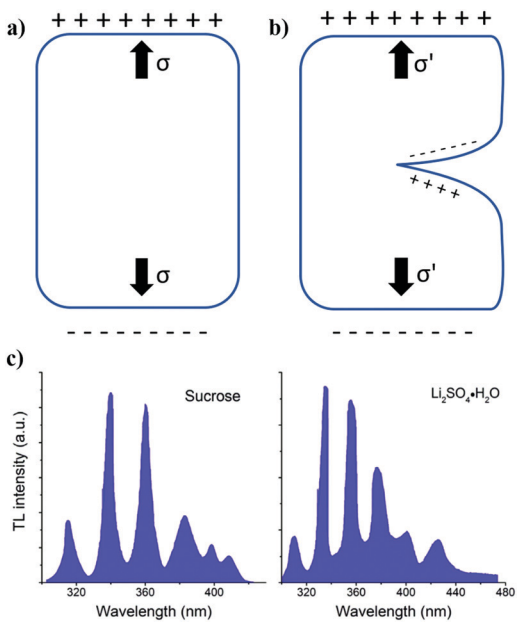

Fig. 2 (a and b) Schematic representations of the mechanism proposed by Langevin. Redesigned from Walton *et al.*, Taylor & Francis.[73] (c) Typical TL spectra of sucrose and $Li_2SO_4{\cdot}H_2O$. Reprinted from Xie *et al.*, Elsevier.[88]

Since TL materials can produce emission without electricity as input, these materials can be used in a wide-range of applications, including mainly sensors and also display technologies,[91,92] emergency lighting, and even biological[93,94] and lighting/solar cell applications.[95–98] In the case of mechanochromic sensor applications, the main purpose is to develop TL material systems that have high durability in terms of producing bright enough optical signals under repeated mechanical actions. First, such a requirement necessitates any selected TL system to exhibit elastic deformation under a corresponding mechanical action that can produce luminescence. Second, this system should also be able to create high brightness while satisfying the above condition. The candidate materials including mechanosensor and surrounding matrix should satisfy the conditions mentioned above. The specific colour rendering of a particular signal makes TL materials functional in composite structures and makes it possible to develop sensors which can simultaneously measure the location and intensity of the mechanical force generated. However, using TL materials alone is not sufficient for impact sensors. This is due to the difficulty in implementation of a TL material, since it is deformed irreversibly and loses its initial crystalline structure. Since the signal is weak, its detection is problematic. Arica *et al.*[57] demonstrated a home-made, unique design of a device to measure both TL and electrical signals when a precise mechanical impact is applied to an EuD_4TEA containing PVDF system under repetitive cycles. Therefore, the incorporation of TL materials into any surrounding system like polymers is, in addition to the requirement of high durability, also crucial for these materials to be used as mechanochromic sensors.

Polymers, as surrounding matrices, can provide significant advantages for TL systems since they exhibit high elastic deformation rates and high durability, protect against the environment and can even improve TL.[99] For instance, Tu *et al.* prepared $Li_xNbO_3{:}Pr^{3+}$ by varying the Li amount and mixed these materials with optical epoxy resin, which were cross-linked through exposure to UV light at 365 nm.[100] They found that slightly Li-rich $Li_xNbO_3{:}Pr^{3+}$ show optimum TL, and the corresponding stress sensors can work in the range from 10^3 Pa to piconewton scales. Qian *et al.* used PDMS as a polymer matrix for ZnS:Mn/Cu@Al_2O_3 microparticles, and they adjusted the elasticity modulus of the composite by employing different amounts and sizes of SiO_2 nanoparticles.[58] Mixing polymers with particles can provide a range of strains under which the

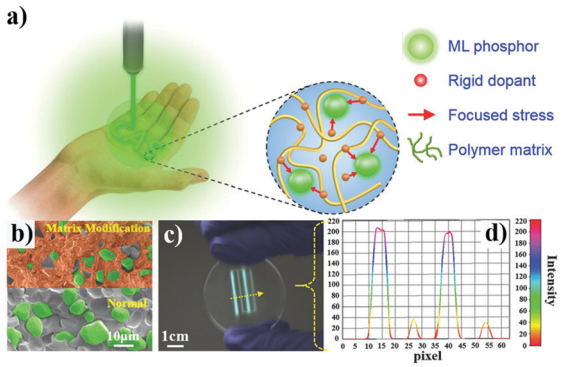

Fig. 3 (a) Schematic demonstration of a flexible device composed of a TL system filled with SiO_2 microparticles. (b) SEM images indicating systems with/without SiO_2, (c) TL under certain stress and (d) TL intensity along the yellow arrow. Reprinted from Qian *et al.*, Wiley.[58]

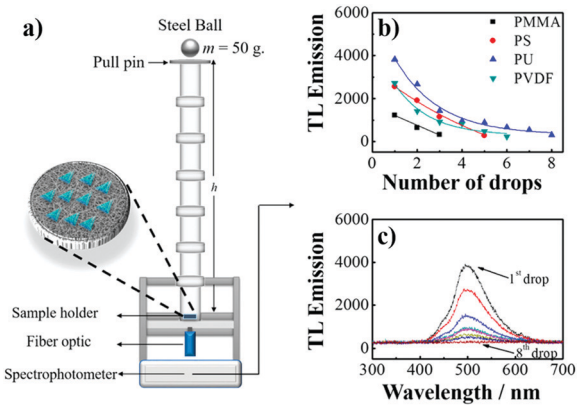

Fig. 4 (a) Drop tower system, (b) TL emission of different polymer mats over varying number of drops, and (c) TL emission of PU fibre mats over varying number of drops. Reprinted from İncel *et al.*, American Chemical Society.[60]

corresponding TL system can work, which can be determined for any specific sensor application. On the other hand, the authors found that the presence of SiO_2 microparticles can also concentrate the stress on the TL material, which can lead to intense luminescent radiation even under weak mechanical actions like stimuli of the moving skin (Fig. 3). This system can be used in flexible and printable devices that may find a wide range of potential applications. For polymer specific investigation of TL performances such as mechanochromic sensors, Incel *et al.* prepared micrometer-sized europium tetrakis(dibenzoylmethide) triethylammonium (EuD_4TEA) crystals and embedded them into various transparent polymers including PMMA, PS, PVDF and PU by either blending in solution or surface impregnation.[59] The main transition of EuD_4TEA was from $^5D_0$ to $^7F_2$. Here, these polymers were selected due to their variation in morphology, and mechanical and electrical properties. PMMA and PS are amorphous, while PVDF and PU exhibit piezoelectric and elastic properties. The authors observed that more than 10% in wt of TL material is needed in order to obtain luminescence when a polymeric film is prepared by casting polymer and TL material dispersion. On the other hand, only 2.5% is required for surface impregnation of TL materials onto polymer films. This conclusion reveals that the preparation method of composites is significant to achieve TL signals. Moreover, among those polymers, surface impregnated PU/TL composites exhibited longer-lived emission and higher TL intensity between applied forces of 2.45 and 42.00 N.

The same group of authors also investigated the TL performance of $Cu(NCS)(py)_2(PPh_3)$ crystals under certain mechanical impacts between 0.98 and 4.98 N, which were measured and applied through a home-made drop tower system presented in Fig. 4a, using the same polymers above but in the form of nonwoven electrospun mats this time.[60] They impregnated the surfaces of these electrospun mats with the corresponding TL material. Similar to their previous study, they found that surface impregnated nonwoven electrospun PU fibres show strong TL response while retaining the difference between the TL and PL emission minima, which may have originated from the chemical affinity between PU and Cu(I). Moreover, in terms of repeatability, the authors observed that using PU fibre mats provides a longer-lived emission that is persistent over a large number of drops, as presented in Fig. 4b and c.

One limitation of TL materials when combined with polymers is the attenuation of luminescence throughout the polymer component. The morphology of polymers plays an important role in sensor materials. Since they usually absorb materials, the intensity of TL rapidly decreases even if the employed polymer is transparent. The application of polymeric fibres as mentioned in the previous example as a substrate for TL crystals did not allow detection of meaningful optical signals. Since the thickness of the fibres is comparable with the wavelength of visible light, the polymer causes rigorous optical scattering of the TL signal.

3 Photoluminescence

Materials that can change their optical fluorescence characteristics upon application of mechanical action have received prominent academic interest and have a wide range of applications from strain sensors to integrated failure indicators. For instance, integrating appropriate organic pigments into ductile or elastic polymer matrices allows fabrication of emissive mechanochromic polymer composites. One of the significant strategies for the fabrication of emissive mechanochromic sensors is based on excimer-forming photoluminescent colour aggregates in a molecularly dissolved/dispersed state that exhibit considerably different emission characteristics. This difference is thought to originate from the formation of nanoscale aggregates of excimer-forming dyes in the polymeric host, which are homogeneously and well distributed under mechanical deformation.[13,29,101,102] Therefore, the force-induced shift in the photoluminescence observed may be irreversible or reversible. As examples, blends of 1,4-bis(α-cyano-styryl)benzenes in poly(ethylene),[103] excimer-forming chromophores or cyano-OPVs,[61,62,103,104] cyano-substituted poly(phenylene ethynylenes),[105] perylenes and perylenebisimides,[106] bis(benzoxazolyl)stilbene,[107]

pyrenes,[108,109] and various polymer matrices[12,29,110] have been used. Besides molecular fluorophores, quantum dots are nanoparticles that can emit PL and have been frequently used for optoelectronic applications. Only the mechanical sensor applications of quantum dots have been reported. Polymer composites have been studied for other stimuli such as temperature and pH.[111–113]

Mechanochromic materials' optical responses through either emitting or shifting emission spectra at certain excitation wavelengths can be explained *via* different mechanisms depending on their morphological properties. During the application of mechanical action, the geometry of photoluminescent compounds may organize throughout the compelled flow direction of the macromolecular matrix. Mainly, the mechanisms of photoluminescent mechanochromic materials can be summarized as aggregation-induced emission/aggregation-caused quenching or aggregation-state transitions such as J-type to H-type and to dimer-type through varying stacking modes of these functionalized molecule crystallizations.[116] Aggregation-induced emission or aggregation-caused quenching can be related to π–π stacking or restricted intramolecular rotation, respectively. Both cases are the consequences of the varying packing formation depending on the corresponding molecule structures. For instance, the π–π stacking of the aggregated molecules can form excimeric shapes that can favour non-radiative decaying channels causing quenching (Fig. 5a), or restricting the rotation of some molecular bonds due to aggregation can release the stored energy radiatively since the rotation is blocked (Fig. 5b). Mechanical stress-induced π–π stacking can lead to transition in the aggregation states, from J-type to H-type and to dimer-type, as the mechanical stress increases (Fig. 5c), which is the inevitable consequence of the strengthened π–π interactions. Such a transition can cause a dramatic red shift in the emission due to excimer formation. Both mechanisms include the formation of excimers, but depending on the molecular structure of the corresponding material, the excimer formation either favours the non-radiative energy decay causing quenching or still decays radiatively but with a lowered energy compared to monomer emission.

Conventional melt-processing techniques are generally used to fabricate physical blends of dyes and host polymers. Crenshaw *et al.* stated that binary mixtures of LLDPE and cyano-OPVs can be readily fabricated by this technique.[61] The homogeneous blends display emission spectra that have been characteristic of the monomer emission of the dyes; however, simple mixing of the components leads to the formation of excimers that emit less energy. The study shows that mechanical deformation can result in a significant change in the emission characteristics of the blends, allowing the excimer deformation framework to be used as a ''molecular'' strain sensor. This result offers tremendous potential for technological applications, especially for the use of polymer artefacts of such dyes as integrated deformation sensors. Fig. 6a shows the chemical structures of the photoluminescent dyes and the emission properties of their mixtures under deformation. These structures are 1,4-bis(*R*-cyano-4-methoxystyryl)-2,5-dimethoxybenzene (BCMDB), 1,4-bis(*R*-cyano-4-methoxystyryl)benzene (BCMB), and 1,4-bis(*R*-cyano-4-(2-ethylhexyloxystyryl))-2,5-dimethoxybenzene (BCEDB). Binary blends of LLDPE and BCMDB or BCMB with a dye concentration of more than 0.18% w/w were prepared by using a twin-screw mini-extruder. Solid state tensile deformation was applied to blend films of LLDPE and 0.18% w/w BCMDB and 0.20% w/w BCMB to

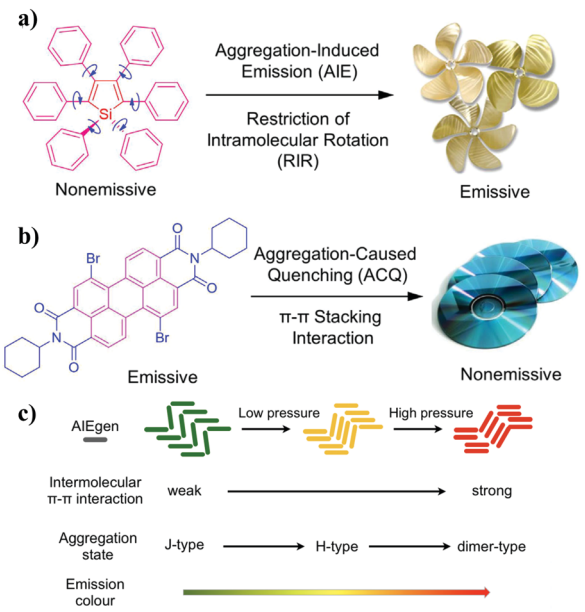

Fig. 5 (a) Propeller-shaped HPS molecules are highly emissive upon aggregation owing to the restriction of intramolecular rotation (RIR) of their multiple phenyl rotors against the silole stator. (b) Disk-shaped DDPD molecules are non-fluorescent in an aggregate state because of the involved strong π–π stacking interaction; reprinted from Wang *et al.*, Elsevier.[114] (c) Schematic diagram of the stacking modes and emission colours with various molecular aggregation states in generic AIE luminogens. Reprinted from A. Pucci, MDPI.[115]

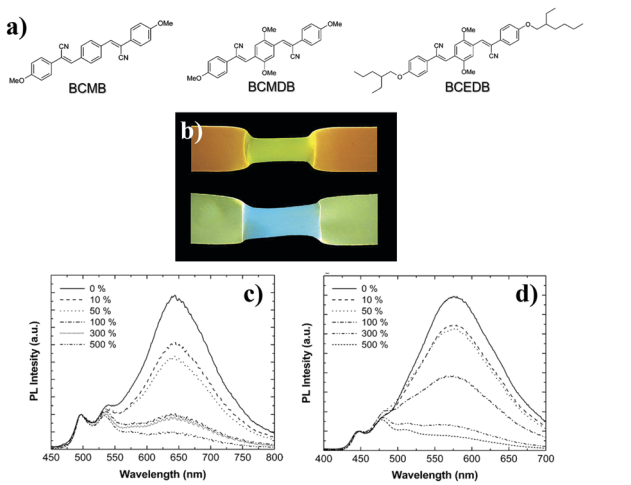

Fig. 6 (a) Chemical structures of photoluminescent dyes employed in this study, (b) photographs of LLDPE and 0.18% w/w BCMDB (top) and 0.20% w/w BCMB (bottom) blend films stretched to 500%, and (c and d) PL emission spectra of blend films of LLDPE with constant dye concentrations of BCMDB and BCMB as functions of stretching ratio. Reprinted from Crenshaw *et al.*, American Chemical Society.[61]

investigate the influence of the deformation on the emission characteristics of the blend films. The mechanical deformation of the materials produced in this way leads to a significant change in the emission colour from green to blue (Fig. 6b). For LLDPE/BCMDB and LLDPE/BCMB blend films, the monomer to excimer emission rate (I_M/I_E) of the unstretched and stretched (500%) samples was compared. This ratio increases approximately 10 times depending on the extend of applied strain. When uniaxial tension was applied to the material, the PL intensity decreased, and a blue shift occurred, probably due to the increase in the I_M/I_E ratio (Fig. 6c and d).[61]

Brent R. Crenshaw and co-workers produced polyethylene blends to investigate deformation-induced colour change in terms of structure–property relationships.[62] The blends of various crystalline ratios of PE and mixtures of two different photoluminescent oligo(phenylene ethylene) dyes were obtained, and colour changes were observed upon mechanical deformation. The cyano-OPVs used in this study were 1,4-bis(α-cyano-4-methoxystyryl)-2,5-dimethoxybenzene (C1-RG) and 1,4-bis(α-cyano-4-octadecyloxystyryl)-2,5-dimethoxybenzene (C18-RG) (Fig. 7a). First, they examined the characteristics of binary mixtures containing C1-RG (previously studied) or C18-RG (0.4% w/w). Both films changed their emission colour from orange to green upon deformation to a strain of 500%. The emission of monomers was observed intensively in the stretched samples and I_M/I_E ratio increased in order of their magnitude. Then, PE94/C18-RG blend films involving between 0.1 and 0.8 percent w/w dye were examined. All films displayed an increase in green monomer fluorescence when stretched (Fig. 7b). The stress–strain profiles for all samples were qualitatively similar, indicating the characteristics of the PE grade.[117] Curiously, the shapes of the I_M/I_E–strain traces, while varying in magnitude between samples, show all similarities to stress–strain profiles that have not been observed to date (Fig. 7c). In addition, the authors also obtained AFM images of a 0.19 w/w PE90/C1-RG blend film before and after deformation (200% strain) (Fig. 7d). According to these AFM phase images, the deformation of the blend films causes the formation of dye crystals. The authors also observed that a large part of the crystalline dye remained as the phase separated from the PE host.

In addition, polyamide structures were shown to exhibit mechanochromic properties when used with excimer forming fluorescent dyes. As another example, low concentrations of (0.15–1 wt%) excimer-forming fluorescent dye, *i.e.* 1,4-bis(α-cyano-4-octadecyloxy styryl)-2,5-dimethoxybenzene (C18-RG), in polyamide 12 were reported as mechanochromic composites.[63] The green fluorescence emission of the monomer gradually shifts to orange excimer fluorescence as the dye concentration increases. This colorimetric change may be due to the fact that well distributed chromophores at low dye concentrations and aggregations produced at high dye concentrations alter the emission properties of the polyamide 12 blends. The structures of polyamide 12 and C18-RG are shown in Fig. 8a. Lavrenova *et al.* also observed a mechanochromic effect at a selected dye concentration (0.25% wt). Depending on the applied force, the materials showed rich monomer emission from excimer dominant fluorescence. Polyamide12/C18-RG materials generated at different concentrations of C18-RG were used at 80% deformation to examine the mechanochromic effect. According to the PL spectra in Fig. 8b, the emission of the monomers is observed at low dye concentrations at approximately 600 nm, while the emission of the excimers is demonstrated at high concentrations. Upon applied deformation, polymer blends containing 0.15% and 0.25% C18-RG displayed a green monomer emission. On the other hand, it was claimed that polymer blends with 0.5% and 1% C18-RG showed orange emission due to the excimer luminescence (Fig. 8c).

Zeng *et al.*[64] were inspired by muscle-controlled surface structures and examined the colour properties of four mechanochromic devices through cracks and folds formed by application of strain. The first device has a reversible transparency change mechanochromic (TCM) effect. The device can display a noticeable visual change between transparent and opaque states when stretched and released within 40% of the strain (Fig. 9a). The authors attributed the opacity of the stretched state to powerful

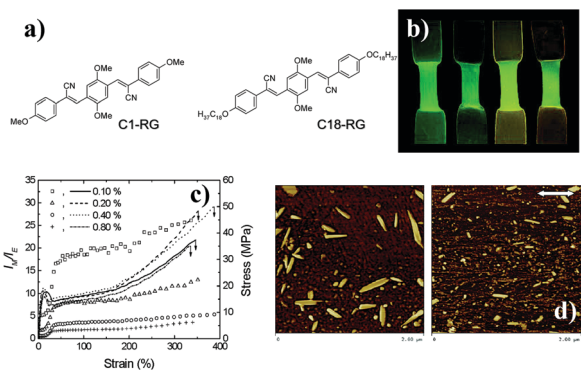

Fig. 7 (a) Chemical structures of cyano-OPVs, (b) photographs of films with approximately 300% strain applied, (c) tensile stress as a function of strain for blends, and (d) AFM images of the free surface of the quenched film before and after deformation. Reprinted from Crenshaw *et al.*, American Chemical Society.[62]

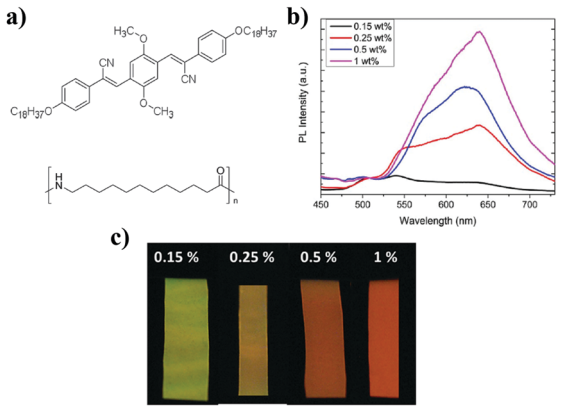

Fig. 8 (a) Chemical structures of excimer-forming dye C18-RG and polyamide 12 included in this study, (b) fluorescence spectra of uniaxially deformed blend films upon stretching 80% with various dye concentrations and (c) photographs. Reprinted from Lavrenova *et al.*, Wiley.[63]

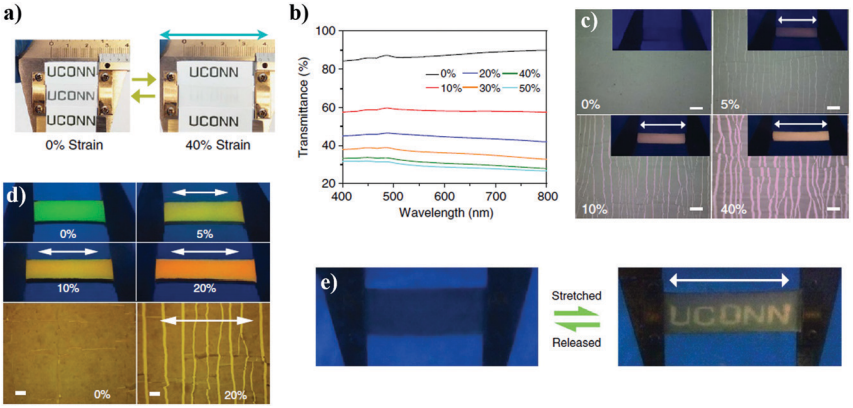

Fig. 9 (a) Photographs of sensitive and reversible TCM stretched at 40% strain, (b) strain dependent transmittance of the TCM, (c) optical microscope images showing the distribution and size of the longitudinal cracks upon stretching in the LM (inset: digital photos of such a device with the corresponding strains under UV light), (d) digital photos of CAM at various strains (0–20%) under UV light, and optical microscope images involve crack size and distribution at the corresponding strain rates, and (e) photograph of the UCONN logo generated in the stretching and releasing cycle by using responsive mechanochromic EM. Reprinted from Zeng *et al.*, Springer Nature.[64]

trapping and light scattering caused by strain-dependent cracks and folds. The optical transmittance *versus* applied strain graphs for the TCM are shown in Fig. 9b. This behaviour was found to be reversible after 450 000 cycles and encourages smart window applications and dynamic optical switches. In the second case, a TiO_2/PVA composite was selected for the luminescent mechanochromic device due to the high refractive index of TiO_2.[118] When 5% stretching was applied, the film did not present visible fluorescence initially, and luminescence was only observed in the presence of cracks. On the other hand, once the film was stretched to 40% of the strain, the system displayed a powerful luminescence (Fig. 9c). Colour alteration mechanochromism (CAM) was explored throughout the third device. The CAM device involved both a green (aponite/fluorescein) thin film of TiO_2/PVA and an orange fluorescent additive (Y_2O_3:Eu_3^+) connected to a PDMS layer. The authors demonstrated that the CAM device could turn the fluorescence from green to orange as it stretched within 20% of the strain (Fig. 9d). As another example, a patterned TiO_2 coating with a 'UCONN' logo was placed on top of the PDMS/carbon black layer to observe the strain responsive sensitivity of encryption mechanochromism (EM). Upon stretching and releasing the sample (0–17% strain) under ultraviolet light, the invisible "UCONN" logo could be reversibly exposed and removed (Fig. 9e).

4. Scattering

In nature, many creatures have stunning structural colours, and some may change their colour in response to environmental stimuli.[18] The mechanism is supposed to change their colour rapidly using their muscles to stretch and tuning their periodic nanostructures.[7,119–121] These adaptive colorations usually play a significant role in camouflage, signal communication, or reproductive behaviour.[122–124] Structural colours arise from the interference, diffraction, and dispersion of light from micro- or nanostructures with distinct sizes in the order of visible light wavelengths. This colouring mechanism provides a promising alternative to dynamically change the material's optical properties in response to external stimuli without altering the chemical or electronic structure of the materials.[125,126]

Colloidal particles have been used in nature to alter the appearance of various species in a variety of ways, mainly based on scattering.[127] In general, the term scattering indicates the interference of light with different wavelengths reflected from scattering objects, either constructively or destructively.[128,129] The colour of an iridescent blue leaf originates from the physical effect, the constructive interference of the reflected blue light.[130,131] Colloidal structures, due to their easy production and versatility, are commonly used to build synthetic photonic materials. Typically, spherical colloidal particles ranging from 100 nm to several μm are made of PS, PMMA, and SiO_2 to produce a photonic impact.[132] Using emulsion polymerization,[133,134] dispersion polymerization,[135] and Stöber[136] processes, these colloids can be synthesized with high accuracy and uniformity, whereas photonic crystals in a colloidal state can be manufactured in much lower costs and with greater efficiencies by using a self-assembly approach. Theoretically, control over coloration may be any means that essentially causes a change in the refractive indices of the building blocks or the surrounding matrix and changes the constants of the lattice or the spatial symmetry of crystalline arrays.[42]

In general, constructive interference due to the periodicity of the framework results in an intense reflection within the stop-band. The thickness of each optical sequence containing high and low refractive indices is expressed as $m\lambda/2n$. The difference in refractive index and the number of periods lead to control over the intensity of the reflected light.[138] More specifically, mechanisms of structural colours can be classified into two categories according to the regularity of their structures, *i.e.* iridescent and non-iridescent. These mechanisms completely rely on the geometry and refractivity of the material.[139] Photonic crystals can be defined as ordered composite structures of materials with different dielectric constants. The relationship between the

wavelength of diffracted light and periodicity is explained by the combination of Bragg's and Snell's laws:

$$\lambda_{max} = 2d_{(111)}\sqrt{(n_{eff}^2 - \sin^2\theta)} \quad (1)$$

It suggests that the diffracted light's wavelength (λ_{max}) is correlated with the incident angle (θ), interplanar distance (d_{111}), and effective refractive index (n_{eff}) of the material (Fig. 10).[140] The interaction of light with a long-range array of colloidal particles contributes to coloration, which normally varies based on the angle of observation (iridescence). Nevertheless, application-based materials require a constant colour that is independent of the viewing angle (non-iridescence), in order to eliminate at least one variable (θ).[141,142] In our previous work, we reported that relatively irregular structures of colloidal SiO_2 particles (quasi-arrays) present non-iridescent structural colours still governed by Bragg–Snell law.[141]

The arrays can retain their optical properties when incorporated into elastic polymer matrices. Therefore, they allow responding to various external stimuli to these materials. Inspired by non-iridescent (angle-independent) natural structural colours, Ge *et al.* fabricated a composite film called a smart optical window embedded in bulk elastomeric PDMS, consisting of a thin layer of a quasi-amorphous SiO_2 nanoparticle array.[65] It was observed that the smart solid window produced was reversibly changed from a highly transparent state (90% permeability in the visible area) to opaqueness (30% transmittance) and reflective colours independent of the screen. The fabrication process of the smart window by a spray method is shown in Fig. 11a. The resulting arrays of bare particles show various colours depending on their particle size (Fig. 11b). According to the SEM image in Fig. 11c, the particle arrays on the PS substrate exhibit quasi-amorphous and short-range ordering. Importantly, since the PDMS refractive index (1.425 at 632.8 nm) is very similar to that of SiO_2 (1.457 at 632.8 nm), the composite film is extremely transparent in the visible and near infrared ranges (Fig. 11d). The colours collected during stretching are blue, green and yellow, based on the various sizes of the SiO_2 particles (Fig. 11f). The shift in optical responses was due to an increase in diffuse light

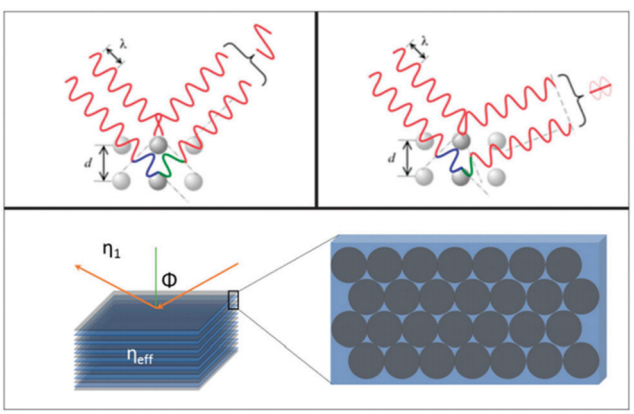

Fig. 10 Interaction of light with periodic materials.[137]

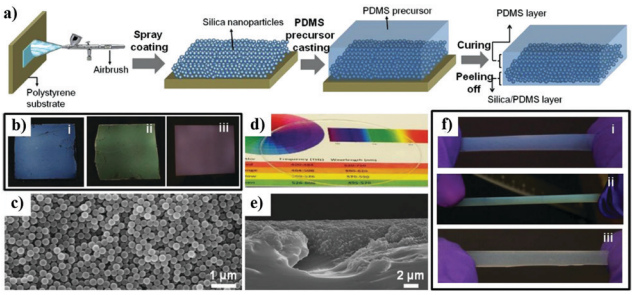

Fig. 11 (a) Fabrication process of smart robust windows, (b) produced structural coloured nano-particle films with various sizes, (c) SEM image of the film displaying quasi-amorphous ordering, (d) digital photograph and (e) SEM image of transparent SiO_2/PDMS composite films, and (f) digital photographs of stretched SiO_2/PDMS films with various sizes of SiO_2 particles. Reprinted from Ge *et al.*, Wiley.[65]

scattering and absorption originating from the creation of micro wrinkles and voids during stretching.

Fudouzi *et al.* described an elastic silicone sheet which has a reversible structural colour.[66] Monodispersed PS particles were used as colloidal particles that embedded in an elastomeric PDMS matrix. When uniaxial stretching was applied to silicone rubber, the lattice parameter decreased in the vertical direction and the reflection signal of the light shifted to a lower wavelength. The colours created due to the mechanical strain applied to the rubber sheet were red and green. Elastic deformation was determined on the basis of the relationship between the initial length and final length of the composite film (Fig. 12a). Fig. 12b shows the reflectance spectra of Bragg's diffraction from the fcc (111) plane of the PDMS rubber sheet. The peak position shows clear shift from higher to lower wavelengths. As a function of mechanical tension, the peak position appears to decrease linearly up to a certain amount of strain (20%) (Fig. 12c). When the mechanical strain on the

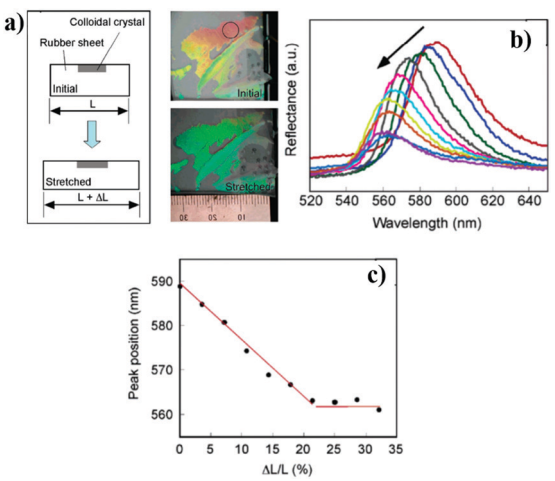

Fig. 12 (a) Elastic deformation until the rubber sheet is stretched from L to $L + \Delta L$ by enforcing mechanical strain and digital images of the rubber sheet before and after deformation, (b) reflectance of the film as a function of wavelength, and (c) peak position as a function of $\Delta L/L$. Reprinted from Fudouzi *et al.*, American Chemical Society.[66]

PDMS sheet was released, the peak returned to its original position. The existing material would be expected to have a wide range of potential applications due to its reversible structural colour properties.

In various applications colloidal crystals have been used to offer strain-induced colour change, or mechanochromism. Lee *et al.*[40] produced chameleon-inspired mechanochromic photonic films composed of non-close packed colloidal arrays. Mechanochromic elastomers contain a non-closed array of SiO_2 particles by mimicking the iridophore structure of chameleons.[7] SiO_2 particles above the threshold volume fraction in the selected rubber precursor were exposed to UV to create a liquid free rubber matrix when they had a regular array. A non-closed colloidal arrangement was thought to cause a large deformation of the elastic matrix, and therefore a complete colour change could be allowed in the absence of colloidal rearrangement. The ordered array produced a colour, and the low difference in refractive index between SiO_2 (n_p = 1.45) and pPEGPEA (n_m = 1.502) enabled the translucency of the films (Fig. 13a). The film cross-section containing a non-close-packed array of SiO_2 particles is shown in the SEM image in Fig. 13b. When 0.20 and 0.47 strains were applied to the film, which had a red colour, it was observed that the film's colour turned green and blue, respectively (Fig. 13c). The films displayed complementary colours with a backlight, as the light was blocked in the stop band, while the light was transmitted from the stop band (Fig. 13d). The authors demonstrated that mechanochromic materials could enable visualization of strain with colours.

Ito and co-workers[41] produced a colloidal crystal film that constitutes monodisperse colloidal particles of a cross-linked random copolymer of MMA and ethyl acrylate prepared by using soap-free emulsion polymerization. The stretched elastomer was found to have a proportional relationship between the peak wavelength and the film thickness. In Fig. 14a, photoimages of the stretched colloid crystal elastomer with various draw ratios are shown. The unstretched film displayed a red colour, and the colour changed to green and blue upon stretching, *i.e.* the colours with shorter wavelengths (Fig. 14b). When the applied strain was removed, the colour changed to red again. The resulting film was thus proven to be recyclable.

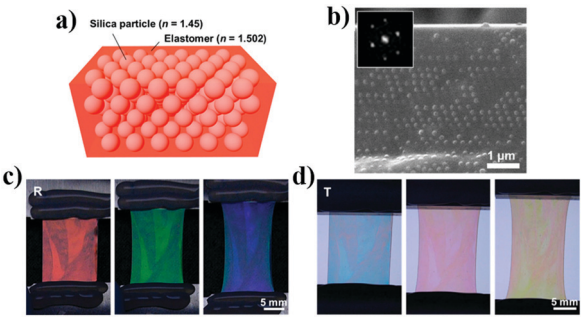

Fig. 13 (a) Schematic of mechanochromic photonic films composed of a non-close-packed array of SiO_2 particles embedded in an elastomeric matrix. (b) SEM image showing the film cross-section containing a non-close-packed array of SiO_2 particles (inset: FFT image). (c and d) Collection of photographs captured in the reflection and transmission of a photonic film with three distinct strains. Reprinted from Lee *et al.*, American Chemical Society.[40]

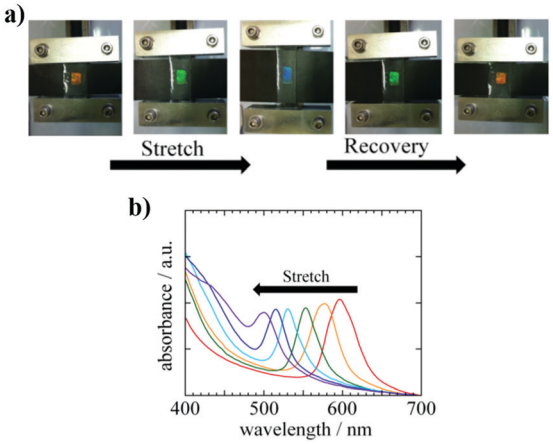

Fig. 14 (a) Digital images of strain-responsive and reversible colloidal crystal elastomers and, (b) their UV-vis absorption spectra. Reprinted from Ito *et al.*, American Chemical Society.[41]

İnci *et al.* produced trilayer colloidal SiO_2 films in elastomeric polyacrylates by using both the Langmuir–Blodgett (LB) deposition technique and photopolymerization process.[39] The self-assembly of colloidal films was prepared by deposition from LB. This technique provided controlled thickness for the colloidal film that had been deposited. After photopolymerization, the generated film has an elastic nature. Thin layer SiO_2 colloidal films displayed iridescent structural colouration. Fig. 15 shows the

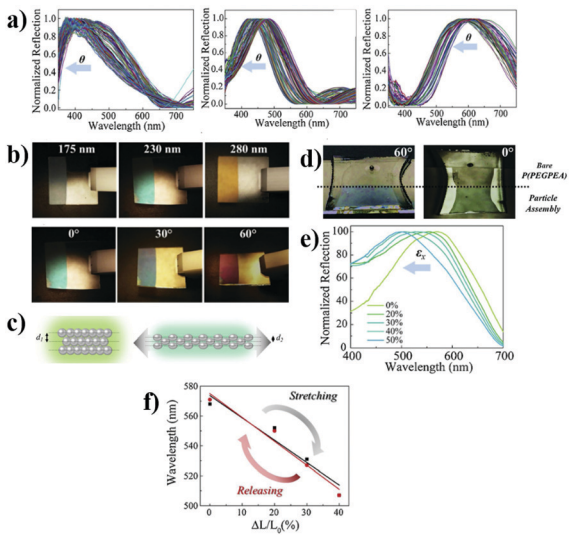

Fig. 15 Colorimetric strain responsive films: (a) normalized reflection spectra of trilayer films consisting of different-sized particles, (b) photographs of their changing iridescent colours by particle size and incident angle, (c) schematic representation of the strain-induced structure change of particle assembly in the elastomer, (d) photographs of an elastomer P(PEGPEA)/SiO_2 composite film with a particle size of 230 nm at various angles, (e) reflection spectra of the composite film having a particle size of 230 nm upon exposure to lateral strain, and (f) change in reflection upon gradual stretching–releasing for reversible optical films. Reprinted from Inci *et al.*, Elsevier.[39]

reflection spectra of trilayer colloidal SiO_2 films with various sizes. The maximum reflection wavelength decreases as the incident angle increases for all spectra. This phenomenon can be explained by the Bragg–Snell law. When viewing the photographs of the structural colour film, bluish, green and yellow colours were observed, respectively, due to the change in the diameter of the particles. Also, iridescence from violet to green (*d*: 230 nm) can also be examined by altering the incident angle (Fig. 15b). Similarly, iridescent green and blue colours were obtained from the composite films prepared by photopolymerization of PEGPEA. The spectrum was recorded such that the maximum of the reflection wavelength shifts to the blue region probably due to the increasing angle (Fig. 15d). The colorimetric response of the material upon stretching depends on both the size of the SiO_2 colloids (due to the changing Bragg diffraction and interplanar distance) and the refractive index difference between the elastomer matrix and the colloids. Not surprisingly, stretching reduces the thickness of the film, resulting in a decrease in the interplanar distance (Fig. 15c). According to Bragg–Snell's law, a decrease in interplanar distance shortens the wavelength of the diffracted light, *i.e.* the colour of the material. A blue shift takes place. Residual strain was completely recovered during stretching and releasing cycles depending on the fixed position of the colloidal particles in the polymer matrix.

5. Plasmonics

Plasmonics deals with interaction of light and matter by governed surface plasmons. Surface plasmon resonance (SPR) refers to electromagnetic beam-induced collective oscillations of the conduction electrons in metallic structures particularly Au and Ag. The oscillations are confined to bulk surfaces or in subwavelength structures, which enables distinct absorption of energy levels, named surface plasmon polaritons (SPPs) and localized SPR (LSPR), respectively. Based on synthesis approaches, both the intensity and the position of the LSPR strongly depend on the geometry and spatial arrangement of metallic nanostructures, as well as the dielectric properties of the surrounding environment.[143–149] Hence, their variable optical properties suggest an alternative remedy for the fabrication of such a mechanical sensor by combining polymeric and plasmonic materials.

The modulation mechanisms of active plasmonic structures are related to controlling the plasmonic materials themselves or their surrounding media. The abundance and diversity of materials employed to design and create functional plasmonic structures and the surrounding media provide great versatility for such plasmonic structures.[150]

The switching of SPR is a direct route toward control of absorbed light. The oscillating electric field from the incident light can couple with the SPR if its momentum matches that of the plasmon. The LSPR can be initiated without requiring complex techniques. The flat dispersion along the wavevector of the incident light (k) allows for excitation of LSPR by incident light over a wide range of angles (Fig. 16a). On the other hand,

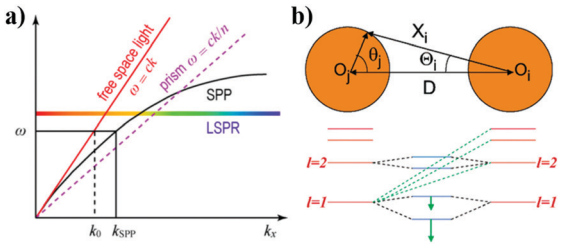

Fig. 16 (a) Dispersion relations of SPP, LSPR, free-space light, and light coupled into a prism, respectively. ω, c, k, and n represent the angular frequency of light, the velocity of light in a vacuum, the propagation constant of light, and the refractive index of the prism, respectively. Reprinted from Maier *et al.*, Springer.[150,151] (b) Schematic picture illustrating the plasmon hybridization in a nanoparticle dimer. Reprinted from Norlander *et al.*, American Chemical Society.[152]

the propagation constant of free-space light is less than that of the SPP. To achieve the desired excitation of the SPP, a momentum transfer may be substantiated by generating attenuated total reflection or diffraction that increases the propagation constant.

To tune the optical transformation of stimuli-responsive plasmonic composites, one can control the interparticle distance. Note that LSPR is particularly sensitive to other adjacent metal nanoparticles. In the case of the proximity of two nanoparticles, their LSPR modes can couple through a near-field interaction, *i.e.* allowing for new modes of plasmon resonance with large enhancements in the electromagnetic field.[149,153] The gap-dependent behaviours of the dipolar coupling in plasmonic dimers, the most basic coupled plasmonic system, can be theoretically described in the scope of the plasmon hybridization model. More specifically, the dipolar plasmon configuration (l = 1) of each individual nanoparticle is split into two characteristic/collective modes, categorized as "bonding" and "antibonding" modes with low and high energy levels, respectively (Fig. 16b). For dimer structures, plasmonic nanospheres with a specified angular momentum interfere with plasmons having a different angular momentum on the other particle at narrow interparticle distances. Several studies in the literature focusing on the gap-dependency have indicated that the fractional plasmon shift ($\Delta\lambda/\lambda_0$) exponentially decays as the interparticle distance increases. Therefore, the proposed equation is given below:

$$\frac{\Delta\lambda}{\lambda_0} = A\mathrm{e}^{\frac{-d}{(s\tau)}} \quad (2)$$

where s is the particle size (*i.e.*, diameter of a nanosphere), τ is defined as the decay length of the electric field from the edge, d is the interparticle gap, and A is the maximal fractional plasmonic shift.[52,154] As a result, the successful regulation of a coupled LSPR compared to an uncoupled one provides the possibilities of extending the tuneable spectrum and benefiting plasmonic responses. With tuneable gap distances of plasmonic metal nanoparticles in liquid or solid media, an external stimulus may undergo reversible interactions,[54,155–157] so that the intensity/duration of the stimulus can be predicted.

"Plasmonic sensors" is a term that refers to systems using spectral changes in the plasmonic connecting system to act as signal transducers.[158] Plasmonic sensors are designed either with nanoparticles supporting LSPR or with 2D chips supporting the SPP mode. Since this text reviews polymeric composite sensor systems, we focus on the discussion of LSPR-based sensors that are typically used. Nanoparticles including Au, Ag, and Cu exhibit size- and dimension-dependent LSPR absorption that make them regular candidates for fabricating plasmonic sensors. A shift in the LSPR's signal can be achieved by the application of an external stimulus that triggers the dis/assembly of the particles resulting in a gap/localization and change in the colour.[159–162] Au NPs differ from other plasmonic additives due to their chemical stability and strong visual changes between blue and red colours readily recognized by the naked eye.

In a flexible matrix, plasmonic nanoparticles can transduce a change in strain/stress within plasmonic spectral signals. The applied strain in a flexible two- or three-dimensional matrix will generate polarized plasmonic spectral signals (Fig. 17). The difference in the strain can be detected visually by shift in absorption characteristics, and therefore in the colour of the polymer composite. Han *et al.* recently developed a colorimetric stress memory sensor, using the disassembly of Au NP aggregates in a mixed PEG and PVP matrix.[67] The change in the plasmonic coupling signal in the absorption spectra of the Au NPs represents the magnitude of the change in the interparticle distance, which indicates the degree of deformation of the film.

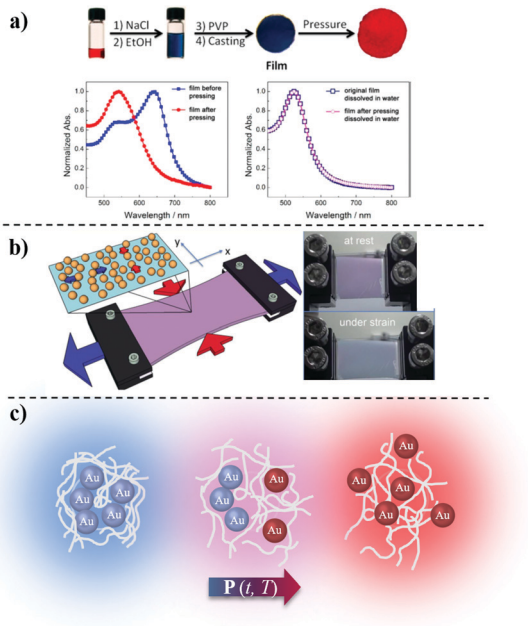

Fig. 17 (a) Preparation of an Au NP based polymeric pressure sensor with colours of different states and the corresponding absorption spectra. Reprinted from Han *et al.*, American Chemical Society.[67] (b) Au NP coated PDMS strain sensor and its reverse colour change due to its dimensional factors. Reprinted from Cataldi *et al.*, Royal Society of Chemistry.[56] (c) Disassembly of Au NPs under pressure in a polymer matrix as a function of time and temperature. Reprinted from Topcu *et al.*, Elsevier.[55]

The distortion of the film depends on stress and length. The colorimetric change and plasmonic shift in response to a variety of stresses are observed by plasticizing the polymer matrix. For instance, our group reported that the embedding of Au NPs into biocompatible and viscoelastic PAAm matrices is a facile route to measure and visualize the applied pressure. The particles in the aqueous state were stabilized by PVP and coagulated until reaching a blue colour in a controlled manner by the addition of PAAm. The blue colour of the film at the initial stage gradually transformed into dark red upon application of pressure. The resulting disc-shaped composite showed distinct sensitivity in the range of 40–160 MPa upon varying the duration of applied pressure.[55] Pressure-sensitive colorimetric PAAm/Au NP composites containing various degrees of crosslinking have also been developed and their sensor properties have been investigated at different relative humidity levels.[163] The change under certain stress depends not only on the degree of force applied but also on internal and external conditions such as the quantity of crosslinking agent and environmental conditions such as temperature and humidity. The change in the topology of polymer chains from linear to crosslinked enables controlling the colour shift due to the fact that dis/integration of the particles in polymer matrices is based on diffusion. The characteristic optical response may allow the use of each crosslinked film as a pressure sensor on different pressure scales. The effect of environmental conditions on sensor properties is not desirable, especially for practical use. Nevertheless, the exposure of the deformed films to intense humidity facilitates the transition back to the initial conditions in both shape and colour. Therefore, this reversible method seems to be a successful route for long-term use of PAAm/Au films.

The mechanical behaviour of composites containing plasmonic particles and polymer matrices is an important parameter that determines the application area of sensor films. The aforementioned polymers including PAAm and PVP are usually known as viscoelastic polymers that continuously undergo deformation under constant force. Therefore, they are useful to determine pressure and its duration, instead of strain measurements due to their irreversible shape recovery without any process. Hence, the mechanical nature of elastomeric matrices such as reversible elasticity is taken as an advantage for the development of plasmonic sensors. For instance, it is reported that interparticle distance is controlled by growth of Au NPs on the PDMS surface and their uniaxial stretching, resulting in a reversible change in sample colour.[56] For a similar purpose, Correa-Duarte *et al.* presented a different method to obtain a polymeric composite of PDMS/Au NPs as a plasmonic transducer based on the deposition of the particles onto the elastomer during stretching.[164] The degree of alignment of plasmonic particles also plays a vital role in also the sensitivity of the plasmonic sensors. In this context, sensors based on a 1D array of Au NPs deposited on PDMS were produced by a combination of water–oil self-assembling and microprinting techniques.[165] The sensitivity of the produced plasmonic grating sensor is around 5.2 ± 0.1 nm/strain% and exhibits a linear behaviour by extending the grating up to 18%

of its original length. Therefore, these abilities make them more sensitive plasmonic strain sensors than those reported in the literature. In the reported plasmonic strain sensors, the colour tends to shift to red. Even though the particles are able to get close/away in 2D, optical characteristics hint that the majority of the particles individualize in the direction of deformation.

The use of nanostructured conductive materials and architectures in combination with polymers can be adapted to both LSPR and SPP, providing excellent potential and versatility for plasmon-enhanced sensor designs. The performance of future plasmon-enhanced sensors relies directly on the successful design of plasmonic architectures and the development of new manufacturing methods. Plasmonics will continue to grow in the future both in developing colorimetric sensors and in building new measurement strategies based on fluorescence and surface-enhanced Raman scattering devices.[166–169]

6. Industrial colorimetric coatings and cost analysis

The coating industry has employed pearl pigments for decorative purposes. The motivation is to bring the illusion of optical depth, angle-dependent eye catching colour effects, and imitation of the effect of natural pearls on various objects.[170] Contrasting from the aforementioned scattering process in structural colours, reflection, multiple reflection, and interference are the main light interaction mechanisms in such pigments. Multilayer films of different refractive indices have been used in most cases. A substrate such as glass or polymer is coated with a high refractive index coating material such as TiO_2 or ZrO_2 to achieve reflection and interference phenomena. Thickness variation is problematic on an industrial scale. This structural variation results in different colour patches. The morphology of pigments is important in light–matter interaction. Particularly, flakes exhibit distinct reflection and cause a sparkling texture in appearance. The colour is found to change with the viewing angle. The origin of this effect lies in the morphology of the pigments. Flakes are two dimensional materials that show an intrinsic anisotropic nature. Thus, the appearance (colour and gloss) varies with the angle. The orientation of the flakes in resulting technology appears to be one of the important structural parameters.[171]

Such a functional polymeric coating system consists of ingredients such as pigments, catalysts, and hardeners. The cost of components depends on application and desired properties. The prominent component in the value chain of a colorimetric product is a mechanochromic additive that is expected to be more advanced than polymeric material. This optically active material may be postulated under the term "pigments" to compare in cost-analysis. Therefore, one can assume that "*pigments*" in this section is not only used for aesthetic appearance but also considering their functional properties such as thermochromism, photochromism, and especially mechanochromism for stimuli-responsive coating systems.[172,173] Smart coatings prepared using such special pigments may be a promising route for the detection of mechanical deformation in transportation or buildings. Particularly, the detection of cracks and delamination is significant because these structural failures in coatings may have consequences regarding passenger safety.

According to Global Market Insights, the global market price of all pigment species in the coating and painting industry is expected to exceed $34 billion by 2020.[174] The Report of Ceresena[175] indicates that the majority of demand in the pigment market is for TiO_2 by almost 60%. The second highest demand is for Fe_3O_4, which is used for colourful pigments. The third is carbon-black mainly used as a filler to increase the mechanical properties of tires. Regarding the mechanochromic additives mentioned in this study, the estimation of their exact price is unambiguous since they are not commercial products. However, the analysis predicts that the prices are not extraordinary for the preliminary industrial trials.

7. Summary and perspectives

In this review, recent advances in the field of colorimetric mechanical sensors based on polymers and mechanochromic additives have been described. Combining polymers and optical recognition units as additives offers a diverse and highly functional approach to the design of flexible colorimetric mechanical sensors, where detection can be done by the naked eye. Compared to commercial mechanochromic sensors usually based on electrical properties (piezoresistivity, capacitance, conductance, *etc.*), colorimetric sensors are advantageous due to the simplicity of component materials without the need for additional equipment for detection. An external mechanical force on the sensor leads to a drastic colour change or sudden luminescence that provides rapid detection. Triboluminescence, photoluminescence, coherent scattering, and LSPR are the underlying mechanisms of this optical alteration in the polymeric matrix. Not surprisingly, the optical mechanism determines the application field of mechanical sensors. For instance, materials showing TL as optical response makes them promising candidates for impact sensors. On the other hand, materials showing photoluminescence and coherent scattering (*i.e.* structural colour) have been widely considered for strain sensor applications. The examples of composites based on plasmonic nanoparticle polymeric matrices as mechanical sensors can be applied to both pressure and strain sensors. The sensor systems inform not only the magnitude but also the distribution of applied external mechanical forces. This feature may be useful for the areas that need rapid detection of mechanical alteration, including construction and transportation. The capability of early recognition by the naked eye makes colorimetric sensors valuable for early detection of failure of various material systems even in construction. The implementation of these colorimetric films still needs to be improved to have saturated colour contrast. Moreover, further efforts on colorimetric polymer composites focused on force-range and stability may improve the reusability of these sensors in daily life.

The encouraging mechanochromic mechanisms reported in this review may contribute to increasing the awareness of colorimetric mechanical sensors. The composites fabricated using polymers and mechanochromic materials exemplified in this review show either reversible or irreversible responses under various intensities and types of mechanical force. Future studies may focus on the development of tailor-made mechanochromic sensors designed for applications requiring more intense optical signals and longer emission lifetimes.

List of abbreviations

Abbreviation or symbol	Definition
λ	Diffraction wavelength
1D	One-dimensional
2D	Two-dimensional
Au	Gold
Au NPs	Gold nanoparticles
BCEDB	1,4-Bis(*R*-cyano-4-(2-ethylhexyloxystyryl))-2,5dimethoxybenzene
BCMB	1,4-Bis(*R*-cyano-4-methoxystyryl)benzene
BCMDB	1,4-Bis(*R*-cyano-4-methoxystyryl)-2,5-dimethoxybenzene
CAM	Colour alteration mechanochromism
Cu	Copper
Cyano-OPV	Cyano-functionalized oligo(phenylenevinylene)
$d_{(111)}$	Interplanar distance
EM	Encryption mechanochromism
EuD_4TEA	Europium tetrakis(dibenzoylmethide) triethylammonium
LB	Langmuir–Blodgett
LLDPE	Linear low-density polyethylene
LM	Longitudinal mechanochromism
Li	Lithium
$Li_xNbO_3:Pr^{3+}$	Lithium niobite
LSPR	Localized surface plasmon resonance
m	Order of diffraction
Mn	Manganese
n	Refractive index
I_m	Intensity of monomer
I_e	Intensity of excimer
PA12	Polyamide 12
PAAm	Poly(acrylamide)
PDMS	Poly(dimethylsiloxane)
PMMA	Poly(methyl methacrylate)
PE	Poly(ethylene)
PEGPEA	Poly(ethylene glycol)phenyl ether acrylate
PEG	Poly(ethylene glycol)
PL	Photoluminescence
PS	Polystyrene
PU	Polyurethane
PVDF	Poly(vinylidene fluoride)
PVP	Poly(vinylpyrrolidone)
SEM	Scanning electron microscope
SERS	Surface-enhanced Raman scattering
SiO_2	Silicon dioxide
SPP	Surface plasmon polariton
SPR	Surface plasmon resonance
TCM	Transparency change mechanochromism
TL	Triboluminescence
TiO_2	Titanium dioxide
UV	Ultraviolet
UV-vis	Ultraviolet-visible
$Y_2O_3:Eu_3^+$	Yttrium oxide, europium-doped
ZnS	Zinc sulfide

Conflicts of interest

There are no conflicts to declare.

References

1 R. A. Crone, *A history of color: the evolution of theories of light and color*, Springer Science & Business Media, 2012.
2 B. McLaughlin, *Colour perception: mind and the physical world*, 2003, pp. 475–502.
3 M. Théry, M. Debut, D. Gomez and J. Casas, *Behav. Ecol.*, 2005, **16**, 25–29.
4 J. A. Endler, *Evolutionary ecology of neotropical freshwater fishes*, Springer, 1984, pp. 95–111.
5 K. R. Elmer, T. K. Lehtonen and A. Meyer, *Evolution*, 2009, **63**, 2750–2757.
6 R. Hanlon, *Curr. Biol.*, 2007, **17**, R400–R404.
7 J. Teyssier, S. V. Saenko, D. Van Der Marel and M. C. Milinkovitch, *Nat. Commun.*, 2015, **6**, 6368.
8 F. Xia and L. Jiang, *Adv. Mater.*, 2008, **20**, 2842–2858.
9 Y. Zhao, Z. Xie, H. Gu, C. Zhu and Z. Gu, *Chem. Soc. Rev.*, 2012, **41**, 3297–3317.
10 H. Fudouzi, *Sci. Technol. Adv. Mater.*, 2011, **12**, 064704.
11 G. Topcu, T. Guner and M. M. Demir, *Ionic Polymer Metal Composites for Sensors and Actuators*, Springer, 2019, pp. 161–182.
12 A. Pucci and G. Ruggeri, *J. Mater. Chem.*, 2011, **21**, 8282–8291.
13 F. Ciardelli, G. Ruggeri and A. Pucci, *Chem. Soc. Rev.*, 2013, **42**, 857–870.
14 B. Z. Tang and A. Qin, *Aggregation-induced emission: applications*, John Wiley & Sons, 2013.
15 C. Weder, *Encyclopedia of Polymeric Nanomaterials*, 2015, pp. 1218–1227.
16 R. J. Tilley, *Colour and the optical properties of materials*, John Wiley & Sons, 2020.
17 A. Choe, J. Yeom, R. Shanker, M. P. Kim, S. Kang and H. Ko, *NPG Asia Mater.*, 2018, **10**, 912–922.
18 R. Zhang, Q. Wang and X. Zheng, *J. Mater. Chem. C*, 2018, **6**, 3182–3199.
19 T. Lu, S. Zhu, Z. Chen, W. Wang, W. Zhang and D. Zhang, *Nanoscale*, 2016, **8**, 10316–10322.

20 V. A. Ganesh, A. Baji and S. Ramakrishna, *RSC Adv.*, 2014, **4**, 53352–53364.
21 P. Bamfield, *Chromic phenomena: technological applications of colour chemistry*, Royal Society of Chemistry, 2010.
22 P. Xue, J. Ding, P. Wang and R. Lu, *J. Mater. Chem. C*, 2016, **4**, 6688–6706.
23 I. R. Howell, C. Li, N. S. Colella, K. Ito and J. J. Watkins, *ACS Appl. Mater. Interfaces*, 2015, **7**, 3641–3646.
24 G. Wegner, M. M. Demir, M. Faatz, K. Gorna, R. Munoz-Espi, B. Guillemet and F. Gröhn, *Macromol. Res.*, 2007, **15**, 95–99.
25 M. M. Demir and G. Wegner, *Macromol. Mater. Eng.*, 2012, **297**, 838–863.
26 J. Hu and S. Liu, *Macromolecules*, 2010, **43**, 8315–8330.
27 D. Chen, J. Yoon, D. Chandra, A. J. Crosby and R. C. Hayward, *J. Polym. Sci., Part B: Polym. Phys.*, 2014, **52**, 1441–1461.
28 L. Zhai, *Chem. Soc. Rev.*, 2013, **42**, 7148–7160.
29 M. W. Urban, *Handbook of stimuli-responsive materials*, John Wiley & Sons, 2011.
30 X. Jin, M. Götz, S. Wille, Y. K. Mishra, R. Adelung and C. Zollfrank, *Adv. Mater.*, 2013, **25**, 1342–1347.
31 S. Shree, M. Dowds, A. Kuntze, Y. K. Mishra, A. Staubitz and R. Adelung, *Mater. Horiz.*, 2020, **7**, 598–604.
32 S. Shree, M. Schulz-Senft, N. H. Alsleben, Y. K. Mishra, A. Staubitz and R. Adelung, *ACS Appl. Mater. Interfaces*, 2017, **9**, 38000–38007.
33 D. O. Olawale, O. O. Okoli, R. S. Fontenot and W. A. Hollerman, *Triboluminescence: theory, synthesis, and application*, Springer, 2016.
34 L. M. Sweeting and A. L. Rheingold, *J. Am. Chem. Soc.*, 1987, **109**, 2652–2658.
35 Y. Sagara and T. Kato, *Nat. Chem.*, 2009, **1**, 605.
36 Y. Hong, J. W. Lam and B. Z. Tang, *Chem. Soc. Rev.*, 2011, **40**, 5361–5388.
37 Z. Chi, X. Zhang, B. Xu, X. Zhou, C. Ma, Y. Zhang, S. Liu and J. Xu, *Chem. Soc. Rev.*, 2012, **41**, 3878–3896.
38 C. I. Aguirre, E. Reguera and A. Stein, *Adv. Funct. Mater.*, 2010, **20**, 2565–2578.
39 E. Inci, G. Topcu and M. M. Demir, *Sens. Actuators, B*, 2020, **305**, 127452.
40 G. H. Lee, T. M. Choi, B. Kim, S. H. Han, J. M. Lee and S.-H. Kim, *ACS Nano*, 2017, **11**, 11350–11357.
41 T. Ito, C. Katsura, H. Sugimoto, E. Nakanishi and K. Inomata, *Langmuir*, 2013, **29**, 13951–13957.
42 J. Ge and Y. Yin, *Angew. Chem., Int. Ed.*, 2011, **50**, 1492–1522.
43 H. Wang and K.-Q. Zhang, *Sensors*, 2013, **13**, 4192–4213.
44 M. Wei, Y. Gao, X. Li and M. J. Serpe, *Polym. Chem.*, 2017, **8**, 127–143.
45 C. Paquet and E. Kumacheva, *Mater. Today*, 2008, **11**, 48–56.
46 E. P. Chan, J. J. Walish, A. M. Urbas and E. L. Thomas, *Adv. Mater.*, 2013, **25**, 3934–3947.
47 S. Enoch, R. Quidant and G. Badenes, *Opt. Express*, 2004, **12**, 3422–3427.
48 P. R. Ohodnicki Jr, C. Wang and M. Andio, *Thin Solid Films*, 2013, **539**, 327–336.
49 B. M. Reinhard, M. Siu, H. Agarwal, A. P. Alivisatos and J. Liphardt, *Nano Lett.*, 2005, **5**, 2246–2252.
50 H. Wang and B. r. M. Reinhard, *J. Phys. Chem. C*, 2009, **113**, 11215–11222.
51 C. Sönnichsen, B. M. Reinhard, J. Liphardt and A. P. Alivisatos, *Nat. Biotechnol.*, 2005, **23**, 741–745.
52 P. K. Jain, W. Huang and M. A. El-Sayed, *Nano Lett.*, 2007, **7**, 2080–2088.
53 I. Pastoriza-Santos, C. Kinnear, J. Pérez-Juste, P. Mulvaney and L. M. Liz-Marzán, *Nature*, 2018, **41578**, 018–0050.
54 I. Tokarev and S. Minko, *Soft Matter*, 2012, **8**, 5980–5987.
55 G. Topcu, T. Guner, E. Inci and M. M. Demir, *Sens. Actuators, A*, 2019, **295**, 503–511.
56 U. Cataldi, R. Caputo, Y. Kurylyak, G. Klein, M. Chekini, C. Umeton and T. Bürgi, *J. Mater. Chem. C*, 2014, **2**, 7927–7933.
57 T. A. Arica, G. Topcu, A. Pala and M. M. Demir, *Measurement*, 2020, **152**, 107316.
58 X. Qian, Z. Cai, M. Su, F. Li, W. Fang, Y. Li, X. Zhou, Q. Li, X. Feng and W. Li, *Adv. Mater.*, 2018, **30**, 1800291.
59 A. İncel, M. Emirdag-Eanes, C. D. McMillen and M. M. Demir, *ACS Appl. Mater. Interfaces*, 2017, **9**, 6488–6496.
60 A. İncel, C. Varlikli, C. D. McMillen and M. M. Demir, *J. Phys. Chem. C*, 2017, **121**, 11709–11716.
61 B. R. Crenshaw and C. Weder, *Chem. Mater.*, 2003, **15**, 4717–4724.
62 B. R. Crenshaw, M. Burnworth, D. Khariwala, A. Hiltner, P. T. Mather, R. Simha and C. Weder, *Macromolecules*, 2007, **40**, 2400–2408.
63 A. Lavrenova, A. Holtz, Y. C. Simon and C. Weder, *Macromol. Mater. Eng.*, 2016, **301**, 549–554.
64 S. Zeng, D. Zhang, W. Huang, Z. Wang, S. G. Freire, X. Yu, A. T. Smith, E. Y. Huang, H. Nguon and L. Sun, *Nat. Commun.*, 2016, **7**, 11802.
65 D. Ge, E. Lee, L. Yang, Y. Cho, M. Li, D. S. Gianola and S. Yang, *Adv. Mater.*, 2015, **27**, 2489–2495.
66 H. Fudouzi and T. Sawada, *Langmuir*, 2006, **22**, 1365–1368.
67 X. Han, Y. Liu and Y. Yin, *Nano Lett.*, 2014, **14**, 2466–2470.
68 M. Waskom, mwaskom/seaborn: v0.8.1 (September 2017) [Internet]. Zenodo, 2017.
69 H. Hofmann, H. Wickham and K. Kafadar, *J. Comput. Graph. Stat.*, 2017, **26**, 469–477.
70 T. L. Dawson, *Color. Technol.*, 2010, **126**, 177–188.
71 J. I. Zink, *Acc. Chem. Res.*, 1978, **11**, 289–295.
72 P. Jha and B. Chandra, *Luminescence*, 2014, **29**, 977–993.
73 A. J. Walton, *Adv. Phys.*, 1977, **26**, 887–948.
74 M. Langevin, *J. Phys. Theor. Appl.*, 1913, **3**, 553–591.
75 H. Longchambon, *CR Acad. Sci. Paris*, 1922, **174**, 1633.
76 H. Longchambon, *C. R. Chim.*, 1923, **176**, 691.
77 J. I. Zink, G. E. Hardy and J. E. Sutton, *J. Phys. Chem.*, 1976, **80**, 248–249.
78 B. Chandra and J. I. Zink, *Inorg. Chem.*, 1980, **19**, 3098–3102.
79 L. M. Sweeting, *Chem. Mater.*, 2001, **13**, 854–870.
80 C. Hurt, N. McAvoy, S. Bjorklund and N. Filipescu, *Nature*, 1966, **212**, 179–180.

81 R. S. Fontenot, K. N. Bhat, W. A. Hollerman and M. D. Aggarwal, *Mater. Today*, 2011, **14**, 292–293.
82 G. Wolff, G. Gross and I. Stranski, *Ber. Bunsen-Ges. Phys. Chem.*, 1952, **56**, 420–428.
83 B. Chandra, *Phys. Status Solidi A*, 1981, **64**, 395–405.
84 B. Chandra and J. I. Zink, *J. Lumin.*, 1981, **23**, 363–372.
85 B. Chandra and J. I. Zink, *J. Phys. Chem. Solids*, 1981, **42**, 529–532.
86 B. Chandra, V. Chandra and P. Jha, *J. Lumin.*, 2013, **135**, 139–153.
87 B. Chandra, V. Chandra, P. Jha, R. Patel, S. Shende, S. Thaker and R. Baghel, *J. Lumin.*, 2012, 132.
88 Y. Xie and Z. Li, *Chemistry*, 2018, **4**, 943–971.
89 Z. Monette, A. K. Kasar and P. L. Menezes, *J. Mater. Sci.: Mater. Electron.*, 2019, 1–16.
90 Z. Wang and F. Wang, *Luminescence – OLED Technology and Applications*, IntechOpen, 2018.
91 J. Zhang, L. Bao, H. Lou, J. Deng, A. Chen, Y. Hu, Z. Zhang, X. Sun and H. Peng, *J. Mater. Chem. C*, 2017, **5**, 8027–8032.
92 S. M. Jeong, S. Song, K.-I. Joo, J. Kim, S.-H. Hwang, J. Jeong and H. Kim, *Energy Environ. Sci.*, 2014, **7**, 3338–3346.
93 Y. Jiang, F. Wang, H. Zhou, Z. Fan, C. Wu, J. Zhang, B. Liu and Z. Wang, *Mater. Sci. Eng., C*, 2018, **92**, 374–380.
94 N. Terasaki, H. Zhang, H. Yamada and C.-N. Xu, *Chem. Commun.*, 2011, **47**, 8034–8036.
95 N. Terasaki, C.-N. Xu, Y. Imai and H. Yamada, *Jpn. J. Appl. Phys.*, 2007, **46**, 2385.
96 S. Moon Jeong, S. Song, S.-K. Lee and B. Choi, *Appl. Phys. Lett.*, 2013, **102**, 051110.
97 S. M. Jeong, S. Song, S. K. Lee and N. Y. Ha, *Adv. Mater.*, 2013, **25**, 6194–6200.
98 S. M. Jeong, S. Song, H. Kim, K. I. Joo and H. Takezoe, *Adv. Funct. Mater.*, 2016, **26**, 4848–4858.
99 R. S. Fontenot, W. A. Hollerman, K. N. Bhat, M. D. Aggarwal and B. G. Penn, *Polym. J.*, 2014, **46**, 111–116.
100 D. Tu, C. N. Xu, A. Yoshida, M. Fujihala, J. Hirotsu and X. G. Zheng, *Adv. Mater.*, 2017, **29**, 1606914.
101 A. Pucci, R. Bizzarri and G. Ruggeri, *Soft Matter*, 2011, **7**, 3689–3700.
102 Y. Sagara, S. Yamane, M. Mitani, C. Weder and T. Kato, *Adv. Mater.*, 2016, **28**, 1073–1095.
103 C. Löwe and C. Weder, *Adv. Mater.*, 2002, **14**, 1625–1629.
104 M. Kinami, B. R. Crenshaw and C. Weder, *Chem. Mater.*, 2006, **18**, 946–955.
105 A. Pucci, T. Biver, G. Ruggeri, L. I. Meza and Y. Pang, *Polymer*, 2005, **46**, 11198–11205.
106 F. Donati, A. Pucci, C. Cappelli, B. Mennucci and G. Ruggeri, *J. Phys. Chem. B*, 2008, **112**, 3668–3679.
107 A. Pucci, M. Bertoldo and S. Bronco, *Macromol. Rapid Commun.*, 2005, **26**, 1043–1048.
108 N. A. Rossi, E. J. Duplock, J. Meegan, D. R. Roberts, J. J. Murphy, M. Patel and S. J. Holder, *J. Mater. Chem.*, 2009, **19**, 7674–7686.
109 D. R. Roberts, M. Patel, J. J. Murphy and S. J. Holder, *Sens. Actuators, B*, 2012, **162**, 43–56.
110 S. A. Jenekhe and D. J. Kiserow, *Chromogenic phenomena in polymers: tunable optical properties*, ACS Publications, 2004.
111 Z. Kang, A. A. Banishev, G. Lee, D. A. Scripka, J. Breidenich, P. Xiao, J. Christensen, M. Zhou, C. J. Summers and D. D. Dlott, *J. Appl. Phys.*, 2016, **120**, 043107.
112 M. Ghannad-Rezaie, L. J.-S. Yang, H. J. Garton and N. Chronis, *J. Microelectromech. Syst.*, 2011, **21**, 23–33.
113 K. Paek, H. Yang, J. Lee, J. Park and B. J. Kim, *ACS Nano*, 2014, **8**, 2848–2856.
114 H. Wang, E. Zhao, J. W. Lam and B. Z. Tang, *Mater. Today*, 2015, **18**, 365–377.
115 M. Kasha, H. R. Rawls and M. A. El-Bayoumi, *Pure Appl. Chem.*, 1965, **11**, 371–392.
116 A. Pucci, *Sensors*, 2019, **19**, 4969.
117 P. Flory, *J. Am. Chem. Soc.*, 1962, **84**, 2857–2867.
118 J. R. DeVore, *J. Opt. Soc. Am.*, 1951, **41**, 416–419.
119 P. Vukusic and J. R. Sambles, *Nature*, 2003, **424**, 852–855.
120 S. V. Saenko, J. Teyssier, D. Van Der Marel and M. C. Milinkovitch, *BMC Biol.*, 2013, **11**, 105.
121 D. G. DeMartini, D. V. Krogstad and D. E. Morse, *Proc. Natl. Acad. Sci. U. S. A.*, 2013, **110**, 2552–2556.
122 D. Gur, B. Leshem, V. Farstey, D. Oron, L. Addadi and S. Weiner, *Adv. Funct. Mater.*, 2016, **26**, 1393–1399.
123 S. A. Kane, Y. Wang, R. Fang, Y. Lu and R. Dakin, *PLoS One*, 2019, **14**, e0210924.
124 H. M. Schaefer, V. Schaefer and D. J. Levey, *Trends Ecol. Evol.*, 2004, **19**, 577–584.
125 S. Kinoshita and S. Yoshioka, *ChemPhysChem*, 2005, **6**, 1442–1459.
126 M. Srinivasarao, *Chem. Rev.*, 1999, **99**, 1935–1962.
127 L. Li, S. Kolle, J. C. Weaver, C. Ortiz, J. Aizenberg and M. Kolle, *Nat. Commun.*, 2015, **6**, 6322.
128 J. Huxley, *Proc. R. Soc. London, Ser. B*, 1976, **193**, 441–453.
129 R. O. Prum, T. Quinn and R. H. Torres, *J. Exp. Biol.*, 2006, **209**, 748–765.
130 D. W. Lee, *Am. Sci.*, 1997, **85**, 56.
131 K. S. Gould and D. W. Lee, *Am. J. Bot.*, 1996, **83**, 45–50.
132 Y. Xia, B. Gates, Y. Yin and Y. Lu, *Adv. Mater.*, 2000, **12**, 693–713.
133 W. D. Harkins, *J. Am. Chem. Soc.*, 1947, **69**, 1428–1444.
134 J. Goodwin, J. Hearn, C. Ho and R. Ottewill, *Colloid Polym. Sci.*, 1974, **252**, 464–471.
135 S. Jiang, E. D. Sudol, V. L. Dimonie and M. S. El-Aasser, *J. Appl. Polym. Sci.*, 2008, **108**, 4096–4107.
136 W. Stöber, A. Fink and E. Bohn, *J. Colloid Interface Sci.*, 1968, **26**, 62–69.
137 E. Armstrong and C. O'Dwyer, *J. Mater. Chem. C*, 2015, **3**, 6109–6143.
138 H. A. Macleod, *Thin-film optical filters*, Institute of Physics Pub, Bristol, UK, 2001.
139 J. Sun, B. Bhushan and J. Tong, *RSC Adv.*, 2013, **3**, 14862–14889.
140 G. A. Ozin and A. Arsenault, *Nanochemistry: a chemical approach to nanomaterials*, Royal Society of Chemistry, 2015.

141 G. Topçu, T. Güner and M. M. Demir, *Photonics and Nanostructures – Fundamentals and Applications*, 2018, 29, pp. 22–29.
142 J. G. Park, S. H. Kim, S. Magkiriadou, T. M. Choi, Y. S. Kim and V. N. Manoharan, *Angew. Chem., Int. Ed.*, 2014, **53**, 2899–2903.
143 E. Ringe, J. Zhang, M. R. Langille, K. Sohn, C. Cobley, L. Au, Y. Xia, C. A. Mirkin, J. Huang and L. D. Marks, *MRS Online Proc. Libr.*, 2009, 1208.
144 E. Ringe, M. R. Langille, K. Sohn, J. Zhang, J. Huang, C. A. Mirkin, R. P. Van Duyne and L. D. Marks, *J. Phys. Chem. Lett.*, 2012, **3**, 1479–1483.
145 P. K. Jain and M. A. El-Sayed, *J. Phys. Chem. C*, 2007, **111**, 17451–17454.
146 D. W. Brandl, N. A. Mirin and P. Nordlander, *J. Phys. Chem. B*, 2006, **110**, 12302–12310.
147 S. K. Ghosh and T. Pal, *Chem. Rev.*, 2007, **107**, 4797–4862.
148 H. Chen, L. Shao, Q. Li and J. Wang, *Chem. Soc. Rev.*, 2013, **42**, 2679–2724.
149 N. J. Halas, S. Lal, W.-S. Chang, S. Link and P. Nordlander, *Chem. Rev.*, 2011, **111**, 3913–3961.
150 N. Jiang, X. Zhuo and J. Wang, *Chem. Rev.*, 2017, **118**, 3054–3099.
151 S. A. Maier, *Plasmonics: fundamentals and applications*, Springer Science & Business Media, 2007.
152 P. Nordlander, C. Oubre, E. Prodan, K. Li and M. Stockman, *Nano Lett.*, 2004, **4**, 899–903.
153 B. Luk'yanchuk, N. I. Zheludev, S. A. Maier, N. J. Halas, P. Nordlander, H. Giessen and C. T. Chong, *Nat. Mater.*, 2010, **9**, 707–715.
154 C. Tabor, R. Murali, M. Mahmoud and M. A. El-Sayed, *J. Phys. Chem. A*, 2009, **113**, 1946–1953.
155 H. Hu, F. Ji, Y. Xu, J. Yu, Q. Liu, L. Chen, Q. Chen, P. Wen, Y. Lifshitz and Y. Wang, *ACS Nano*, 2016, **10**, 7323–7330.
156 Z. Sun, W. Ni, Z. Yang, X. Kou, L. Li and J. Wang, *Small*, 2008, **4**, 1287–1292.
157 Y. Liu, X. Han, L. He and Y. Yin, *Angew. Chem., Int. Ed.*, 2012, **51**, 6373–6377.
158 M. Li, S. K. Cushing and N. Wu, *Analyst*, 2015, **140**, 386–406.
159 T. Kim, K. Lee, M.-S. Gong and S.-W. Joo, *Langmuir*, 2005, **21**, 9524–9528.
160 L. He, M. D. Musick, S. R. Nicewarner, F. G. Salinas, S. J. Benkovic, M. J. Natan and C. D. Keating, *J. Am. Chem. Soc.*, 2000, **122**, 9071–9077.
161 H. Liang, H. Zhao, D. Rossouw, W. Wang, H. Xu, G. A. Botton and D. Ma, *Chem. Mater.*, 2012, **24**, 2339–2346.
162 H. N. Kim, W. X. Ren, J. S. Kim and J. Yoon, *Chem. Soc. Rev.*, 2012, **41**, 3210–3244.
163 G. Topcu and M. M. Demir, *Sens. Actuators, A*, 2019, **295**, 237–243.
164 M. A. Correa-Duarte, V. Salgueiriño-Maceira, A. Rinaldi, K. Sieradzki, M. Giersig and L. M. Liz-Marzán, *Gold Bull.*, 2007, **40**, 6–14.
165 L. Minati, A. Chiappini, C. Armellini, A. Carpentiero, D. Maniglio, A. Vaccari, L. Zur, A. Lukowiak, M. Ferrari and G. Speranza, *Mater. Chem. Phys.*, 2017, **192**, 94–99.
166 V. Giannini, A. I. Fernández-Domínguez, S. C. Heck and S. A. Maier, *Chem. Rev.*, 2011, **111**, 3888–3912.
167 H. Li, C.-Y. Chen, X. Wei, W. Qiang, Z. Li, Q. Cheng and D. Xu, *Anal. Chem.*, 2012, **84**, 8656–8662.
168 H. Kang, C.-J. Heo, H. C. Jeon, S. Y. Lee and S.-M. Yang, *ACS Appl. Mater. Interfaces*, 2013, **5**, 4569–4574.
169 K. D. Alexander, K. Skinner, S. Zhang, H. Wei and R. Lopez, *Nano Lett.*, 2010, **10**, 4488–4493.
170 F. J. Maile, G. Pfaff and P. Reynders, *Prog. Org. Coat.*, 2005, **54**, 150–163.
171 I. Wheeler, *Metallic pigments in polymers*, iSmithers Rapra Publishing, 1999.
172 C. Deya, R. Romagnoli and B. Del Amo, *J. Coat. Technol. Res.*, 2007, **4**, 167–175.
173 K. Yamada, Y. Yamagishi, T. Ayabe, S.-H. Son, M. Aoyagi and T. Taira, *US Pat.*, US20120015399A1, 2012.
174 C. Diamond, Pigments Market Update, https://www.coatingsworld.com/issues/2016-01-01/view_features/pigments-market-update-667201/, accessed 08.05.2020.
175 Paints and Coatings Market Report – Europe, https://www.ceresana.com/en/market-studies/industry/paints-coatings-europe/market-study-on-paints-coatings-europe.html.